JOURNAL OF Materials CHEMISTRY

Magnetic properties of two hydrothermally synthesized iron(III) phosphates: $Fe(NH_3)_2PO_4$ and $Fe(NH_4)(HPO_4)_2$

Aintzane Goñi,[a] Luis Lezama,[a] Aránzazu Espina,[b] Camino Trobajo,[b] José R. García[b] and Teófilo Rojo*[a]

[a]*Departamento de Química Inorgánica, Facultad de Ciencias, UPV/EHU, Aptdo. 644, 48080 Bilbao, Spain*
[b]*Departamento de Química Orgánica e Inorgánica, Universidad de Oviedo, 33006 Oviedo, Spain*

Received 17th May 2001, Accepted 30th May 2001
First published as an Advance Article on the web 26th July 2001

The open-framework compounds $Fe(NH_3)_2PO_4$ and $Fe(NH_4)(HPO_4)_2$ were synthesized by hydrothermal reactions in the H_3PO_4–$(NH_2)_2CO$–$FeCl_3$–H_2O system. The electron paramagnetic resonance spectra for $Fe(NH_3)_2PO_4$ show an isotropic signal with $g=2$, characteristic of high spin Fe(III) ions in an octahedral environment. Below 22 K the $Fe(NH_3)_2PO_4$ compound exhibits a long-range antiferromagnetic ordering in which the magnetic interactions involve Fe–O–P–O–Fe superexchange pathways. $Fe(NH_4)(HPO_4)_2$ exhibits an antiferromagnetic behaviour with the presence of a significant ferromagnetic component from 18 to 3 K. In this temperature range one component of the resonance signal undergoes a shift from 336 mT ($g=2$) toward magnetic fields near to zero, indicating the existence of low-dimensional ferromagnetic interactions. The presence of that ferromagnetic component was attributed to the frustration of one third of the total Fe(III) spins in the compound. Below 3 K, the effect of the long-range interactions causes an antiparallel arrangement of the magnetic moments inducing another magnetic transition to an antiferromagnetic phase.

Introduction

The field of open-framework inorganic materials has experienced a dramatic increase over the past years. These materials can be used as catalysts, ion exchangers, in sensors and in nanotechnology.[1] The iron phosphates have opened the way to a new class of open-framework solids that combine the well-known sieving properties with interesting magnetic properties.[2,3] The most striking example is provided by the mineral cacoxenite[4] $[AlFe_{24}(OH)_{12}(PO_4)_{17}(H_2O)_{24}]\cdot 51H_2O$. This compound, together with the synthetic materials described by Corbin *et al.*,[5] has opened the way for the attainment of new iron phosphates with interesting applications.[6–9] Concerning the magnetic properties of these materials, despite the existence of isolated clusters linked by phosphate groups, three-dimensional magnetic ordering takes place over a wide range of temperatures, with either antiferro-, weak ferro- or ferrimagnetic properties.[10]

There are many solids with potentially very large cavities whose structures collapse in the absence of pore-filling species.[11] So, in several open-framework iron phosphates the empty space is filled by loosely bound guest species such as organic molecules, water or ammonia. In this sense, the $FeCl_3$–H_3PO_4–$(NH_2)_2CO$–H_2O system[12] has provided some interesting phases synthesized from hydrothermal reactions, for example, the well-known spheniscidite mineral $NH_4[Fe_2(PO_4)_2(OH)H_2O]H_2O$,[13–15] the special compound $Fe(NH_3)_2PO_4$,[16] in which the ammonia molecules coordinate to the Fe(III) ions, and the ammonium–iron(III) bis(hydrogenphosphate), $Fe(NH_4)(HPO_4)_2$.[17] These phases do not show strictly microporous structures, owing to the small size of their cavities; however, the magnetic behaviour of these compounds is quite interesting. In this way, the spheniscidite mineral exhibits three-dimensional magnetic exchange interactions. The structure of this compound[18] permits the existence of a strongly frustrated magnetic configuration because of the competition between the antiferromagnetic interactions present in the compound.

The $Fe(NH_3)_2PO_4$ phase is structurally related to $Fe(H_2O)_2PO_4$. This compound presents two forms, strengite and metastrengite, the latter also named phosphosiderite.[19] The three-dimensional structure of $Fe(NH_3)_2PO_4$ is built by isolated iron octahedra linked together by phosphate tetrahedra [see Fig. 1(a)]. Two ammonia molecules are coordinated to each Fe(III) ion appearing at the ends of an octahedral edge and at the same positions as the water molecules in strengite. So, the structural formula for the octahedra can be written as *cis*-$Fe(N)_2(O)_4$, where the oxygen belongs to the phosphate group and the nitrogen is from the ammonia molecules.

The $Fe(NH_4)(HPO_4)_2$ compound is structurally related to $(Al_{0.64}Ga_{0.36})(NH_4)(HPO_4)_2$[20] but is quite different from $Fe(H_3O)(HPO_4)_2$.[21] The structure can be described as a three-dimensional framework of corner-sharing FeO_6 octahedra and PO_4 tetrahedra [see Fig. 1(b)]. Each FeO_6 octahedron is surrounded by six PO_4 polyhedra, and each PO_4 tetrahedron is linked to four FeO_6 polyhedra. The ammonium ions lie in the remaining tunnels along [100] and [010] directions, being linked to the three-dimensional network by hydrogen bonds. It is worth mentioning the presence of two independent crystallographic positions for the Fe(III) magnetic ions, Fe(1) and Fe(2), where the occupation factor for the Fe(2) site is twice that corresponding to the Fe(1) site.

Here, we report on the magnetic study of the hydrothermally synthesized $Fe(NH_3)_2PO_4$ and $Fe(NH_4)(HPO_4)_2$ phases. The results show interesting magnetic behaviour provided by Fe–Fe superexchange interactions which are established through the phosphate groups.

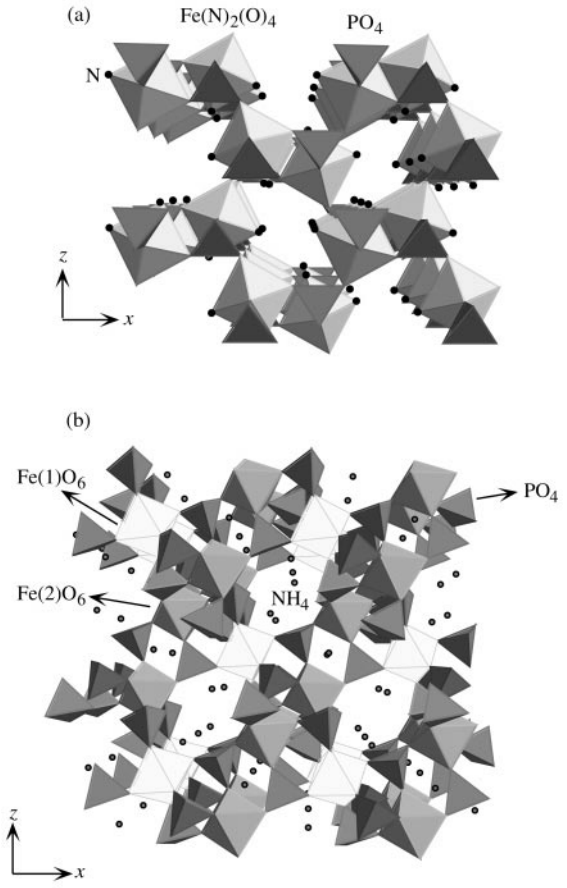

Fig. 1 Crystal structures of (a) $Fe(NH_3)_2PO_4$ and (b) $Fe(NH_4)(HPO_4)_2$.

Experimental

Synthesis

The samples were prepared as described in ref. 12. The differences in the experimental conditions required to obtain $Fe(NH_3)_2PO_4$ and $Fe(NH_4)(HPO_4)_2$ compounds lie basically in the P : Fe ratio and pH value used. The analytical data of both samples were consistent with their composition. Anal. calc. (Found) for $Fe(NH_3)_2PO_4$: Fe, 30.23 (30.2); P, 16.77 (16.8); N, 15.14% (15.2%). Anal. calc. (Found) for $Fe(NH_4)(HPO_4)_2$: Fe, 21.02 (21.4); P, 23.32 (23.1); N, 5.26% (5.2%).

Physico-chemical measurements

Microanalytical data (C, H and N) were obtained with a Perkin-Elmer Model 2400B elemental analyzer. The phosphorus and iron contents of the solids were determined using a Spectrometer DCP-AEC after dissolving the samples in HF(aq). The EPR spectra were recorded on powdered samples at X-band frequency, using a Bruker ESP300 spectrometer equipped with standard Oxford low-temperature devices and calibrated by an NMR probe for the magnetic field. The frequency was measured with a HP 5352B microwave frequency counter. The magnetic measurements in the 1.8–300 K temperature range were performed at different magnetic fields with a Quantum Design MPMS-7 SQUID magnetometer.

Results

Magnetic study on $Fe(NH_3)_2PO_4$

The powder X-band EPR spectra of $Fe(NH_3)_2PO_4$ were measured at different temperatures from 290 to 4.2 K. Selected spectra are shown in Fig. 2. An isotropic signal with a g value of 2.0 is observed at room temperature indicating the presence of high spin Fe^{3+} ions.[22–24] No significant variation of the g value is observed in the spectra obtained over the entire temperature range. These results are in good agreement with those observed for other Fe(III) ions in FeO_6 octahedra.[25–27] As far as we are aware, $Fe(NH_3)_2PO_4$ is the first phosphate compound with $Fe(N)_2(O)_4$ octahedra and the EPR results do not undergo significant changes.

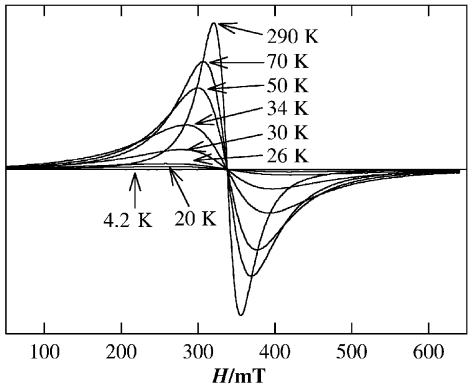

Fig. 2 Selected EPR spectra of $Fe(NH_3)_2PO_4$ at different temperatures.

The thermal evolution of the linewidth of the EPR signal, ΔH_{pp}, calculated by simulations of the experimental spectra of $Fe(NH_3)_2PO_4$ to Lorentzian curves, is displayed in Fig. 3. The linewidth is observed to have low-temperature dependence between RT and 70 K. This fact is probably due to the compensation of the dipolar homogeneous broadening with the exchange narrowing. Below this temperature the linewidth increases rapidly when the temperature decreases, reaching a maximum at 20 K. The intensity of the signal, I, increases slightly with decreasing temperature from 290 down to 65 K where a rounded maximum is reached. After that, the intensity drops to zero with decreasing temperature. This behaviour indicates the existence of magnetic interactions in $Fe(NH_3)_2PO_4$ with a completely ordered state below 20 K.

The study of the thermal evolution of the molar magnetic susceptibility in $Fe(NH_3)_2PO_4$ was carried out in the 5–300 K temperature range with a magnetic field of 0.1 T. The χ_m and $\chi_m T$ *vs.* T curves are shown in Fig. 4. A maximum centred at 28 K is observed in the curve corresponding to the magnetic susceptibility. This fact, together with the thermal evolution of the $\chi_m T$ product, indicates the existence of antiferromagnetic interactions. At high temperatures ($T > 150$ K) the data follow a Curie–Weiss law with a Curie constant of $C_m = 4.45\ cm^3\ K\ mol^{-1}$ and a Weiss temperature of $\theta \approx -70$ K. The g value derived from the calculated Curie constant is 2.01, in

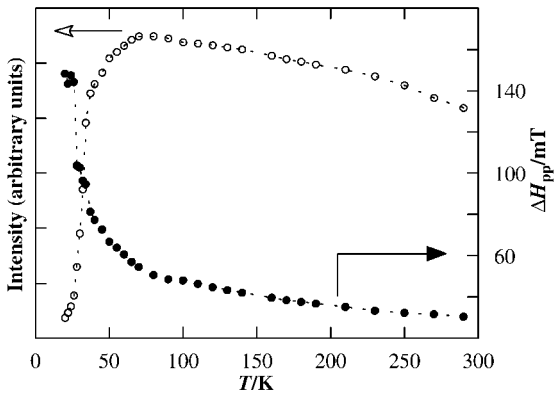

Fig. 3 Thermal evolution of the intensity (I) and the linewidth (ΔH_{pp}) of the EPR signal for $Fe(NH_3)_2PO_4$.

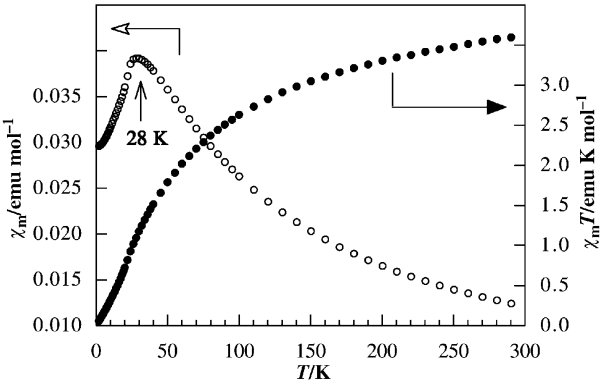

Fig. 4 χ_m and $\chi_m T$ *vs.* temperature for $Fe(NH_3)_2PO_4$ in the 1.8–300 K range at a magnetic field of 0.1 T.

good agreement with the EPR results. The effective magnetic moment calculated from the $\chi_m T$ value at 300 K is 5.37 μ_B. This value is slightly lower than the theoretical one for a high spin Fe(III) ion and can be expected due to the presence of antiferromagnetic interactions. The thermal evolution of the $-d(\chi_m T)/dT$ curve shows a sharp peak at the critical temperature providing a $T_N = 22$ K. The $|\theta/T_N|$ value largely exceeds unity, indicating the presence of an important degree of magnetic frustration, probably resulting from competing interactions.

Magnetic study on $Fe(NH_4)(HPO_4)_2$

The X-band EPR spectra of the $Fe(NH_4)(HPO_4)_2$ polycrystalline sample were recorded in the temperature range 4.2–300 K, and are shown in Fig. 5. All spectra above 30 K exhibit a unique isotropic signal with Lorentzian line shape corresponding to a g value of 2.0. The results obtained at high temperatures are in good agreement with the presence of high spin Fe(III) (^{6}S) ions in octahedral coordination. The good fitting of the Lorentzian derivative to the experimental EPR signals suggests that the magnetic exchange interactions predominate over the dipolar ones. The thermal evolution of both the integrated intensity (I) and linewidth (Γ) is represented

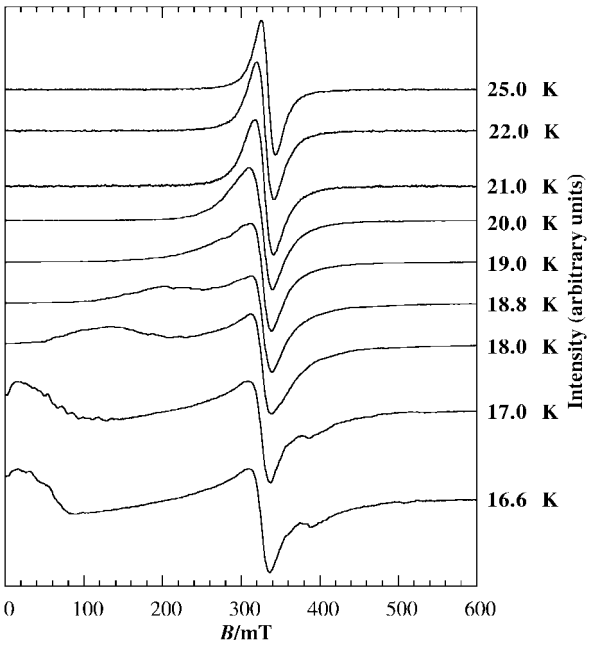

Fig. 5 Selected EPR spectra of $Fe(NH_4)(HPO_4)_2$ at different temperatures.

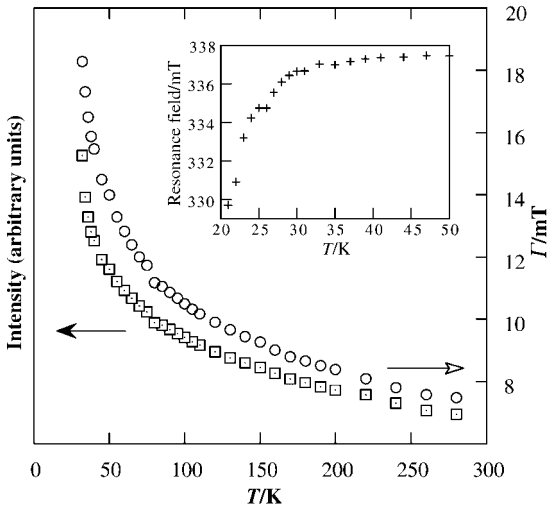

Fig. 6 Thermal evolution of the integrated intensity (I) and linewidth (Γ) of the EPR signals for $Fe(NH_4)(HPO_4)_2$. Inset: resonance field values *vs.* temperature below 50 K.

in Fig. 6. These parameters exhibit similar behaviour, showing moderate thermal dependence at higher temperatures and a quite rapid increase of their values below 50 K, which is indicative of approaching the critical point.

The spectra at lower temperatures are complex, as can be observed in Fig. 5. The resonance field of the isotropic signal undergoes a decrease at temperatures lower than 30 K (see inset in Fig. 6). Moreover, below 21 K the EPR signal loses its isotropic character showing a rapid displacement for one of the g values toward lower resonance fields (see Fig. 5). This component reaches a value near to zero field at 17 K. The quick displacement causes a broadening of the band which hampers the accurate determination of the position of the signal and other parameters such as intensity and linewidth. This phenomenon clearly indicates the appearance of low-dimensional interactions of ferromagnetic nature in the sample. Finally, no resonance is detected at 4.2 K which can be attributed to the establishment of a long-range magnetic order in the compound around that temperature.

The thermal evolution of the molar susceptibility, χ_m, and $\chi_m T$ for $Fe(NH_4)(HPO_4)_2$ at a magnetic field of 0.1 T, are represented in Fig. 7. The χ_m *vs.* T curve shows a strong increase of the magnetic susceptibility below 20 K, reaching a maximum at 4 K. Below this temperature the curve drops to zero. The high temperature data ($T > 150$ K) are well described

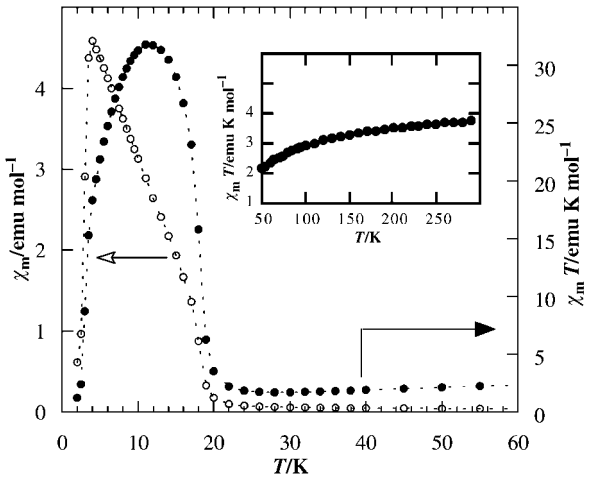

Fig. 7 Thermal evolution of the χ_m and $\chi_m T$ for $Fe(NH_4)(HPO_4)_2$ from 1.8 to 300 K, at 0.1 T.

by a Curie–Weiss law with a Weiss temperature $\theta \approx -50$ K which indicates the predominance of antiferromagnetic interactions. The calculated value for the effective magnetic moment per iron atom is in good agreement with the theoretical value for a high spin Fe(III) ion, 5.92 μ_B. The μ_{eff} obtained from the observed $\chi_m T$ value at room temperature is slightly lower, 5.5 μ_B, which is characteristic of antiferromagnetic compounds.

The $\chi_m T$ product decreases with decreasing temperature from 300 K (see inset in Fig. 7), exhibiting a minimum at 20 K, and then increases very rapidly up to a maximum centred at 11 K. Below this temperature the value of the magnetic effective moment decreases again toward zero. This behaviour indicates the existence of antiferromagnetic interactions with the presence of an important ferromagnetic component. The sharp peak in $-\mathrm{d}(\chi_m T)/\mathrm{d}T$ *vs.* T provides a $T_N = 18.0$ K.

To analyze the ferromagnetic component, magnetization *vs.* field curves were registered in the 25–4 K temperature range (Fig. 8). The compound does not exhibit a magnetic behaviour as could be expected for a pure ferromagnetic system. The magnetization undergoes a quasi-saturation for a magnetic field at around 1 T. However, the saturation is not completely reached in the temperature range studied. In all cases the magnetic moment tends to saturate to values less than 1.7 $\mu_B\,mol^{-1}$. This value is significantly lower than that corresponding to one Fe(III) ion ($S = 5/2$; 5.0 μ_B) per mol of compound. The 1.7 $\mu_B\,mol^{-1}$ value corresponds to approximately one third of the Fe(III) ions per mol. In this sense, the absence of saturation is clearly related to the existence of antiferromagnetic interactions in the compound with an incomplete compensation of spins.

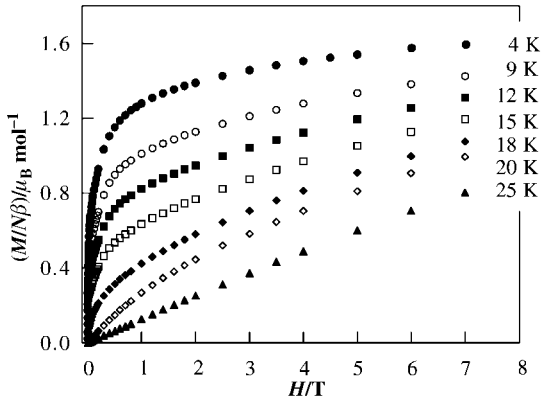

Fig. 8 Magnetization *vs.* field curves of $Fe(NH_4)(HPO_4)_2$ at different temperatures.

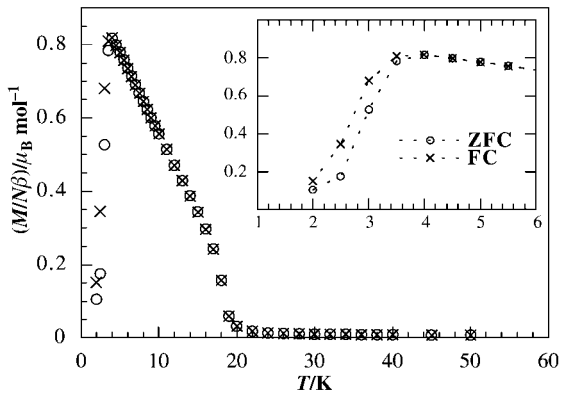

Fig. 9 Molar magnetic susceptibility measurements corresponding to zero field-cooled and 0.1 T field-cooled $Fe(NH_4)(HPO_4)_2$ samples.

Field cooling (FC) and zero field cooling (ZFC) measurements were carried out in the 1.8–50 K temperature range using a magnetic field of 0.1 T. The results are shown in Fig. 9. Similar curves were obtained in both cases above 4 K. Below this temperature a small divergence between ZFC and FC values was observed (see inset in Fig. 9). The small remanent magnetization below 4 K in the field-cooled sample indicates that the magnetic behaviour of $Fe(NH_4)(HPO_4)_2$ undergoes a magnetic transition to an antiferromagnetic phase at low temperatures.

Discussion and conclusion

The Fe–Fe magnetic interactions in both the $Fe(NH_3)_2PO_4$ and $Fe(NH_4)(HPO_4)_2$ compounds are established through the PO_4 groups involving Fe–O–P–O–Fe superexchange pathways.

The $Fe(NH_3)_2PO_4$ phase presents a unique crystallographic site for the iron ions. The $Fe(N)_2(O)_4$ octahedra are arranged in six-membered rings [see Fig. 1(a)] which are packed in the three dimensions of space, leaving tunnels along the y direction. The metallic arrangement allows the establishment of antiferromagnetic interactions of long-range order between the Fe(III) ions leading to the observed three-dimensional antiferromagnetic behaviour.

In the case of $Fe(NH_4)(HPO_4)_2$, there are two independent crystallographic positions for the Fe(III) ions in the unit cell, Fe(1) and Fe(2). This fact allows the existence of two different magnetic sub-lattices, as in the case of $Li_3Fe_2(PO_4)_3$ (see ref. 23). It is important to note that the number of equivalent positions for the Fe(2) site is twice that corresponding to the Fe(1) site. So, there are two interacting Fe(2) for each Fe(1) in the compound (Fig. 10). Considering the values of the angles corresponding to the Fe–O–P–O–Fe exchange pathways (Table 1) and according to Goodenough's rules,[28] the interactions in this compound are expected to be antiferromagnetic.

If we consider J_{12} and J_{22} as the magnetic coupling constants of the Fe(1)–Fe(2) and Fe(2)–Fe(2) superexchange interactions, respectively, three different magnetic spin systems can be proposed. (i) When $|J_{22}| > |J_{12}|$, with all antiferromagnetic interactions (AF), the Fe(1) spins should adopt a non-collinear configuration to minimize frustration effects. (ii) When $|J_{12}| > |J_{22}|$ with AF, the Fe(2)–Fe(2) antiferromagnetic interactions would be frustrated because the Fe(2) magnetic moments should adopt a parallel ordering. Such behaviour was previously observed in another related ammonium iron(III) phosphate, spheniscidite.[29] And finally (iii) considering $J_{22} > 0$ (even if very rare) and $J_{12} < 0$, the same disposition of the spins would occur. In this case, no frustration effects would appear.

The experimental magnetic behaviour observed in the $Fe(NH_4)(HPO_4)_2$ phase is in good agreement with the above proposed spin systems in which the antiferromagnetic interactions are predominant but with a ferromagnetic component in the 18–3 K temperature range. This ferromagnetic moment must be interpreted as a consequence of the magnetic frustration corresponding to one third of the Fe(III) spins. At lower temperatures, the long-range magnetic interactions induce another magnetic transition to a pure antiferromagnetic phase in which all spins are arranged antiparallel to one another.

Acknowledgements

This work has been carried out with the financial support of the Ministerio de Educación y Ciencia (PB97-0640), the UPV/EHU (UPV 169.310-EB149/98), the Comisión Interministerial de Ciencia y Tecnología and the European Commission (MAT97-1185, 1FD97-1965), which we gratefully acknowledge.

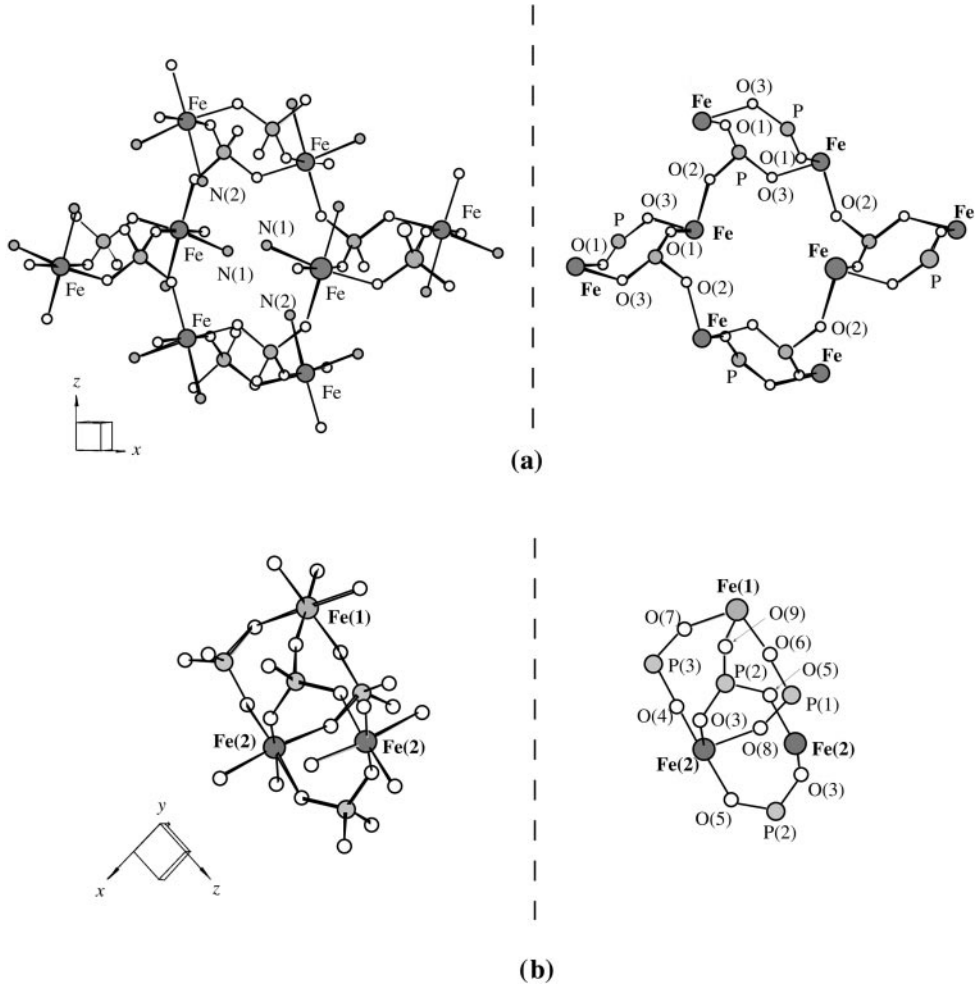

Fig. 10 Scheme of the magnetic exchange pathways in (a) $Fe(NH_3)_2PO_4$ and (b) $Fe(NH_4)(HPO_4)_2$.

Table 1 Selected angles of the Fe–O–P–O–Fe magnetic exchange pathways for the $Fe(NH_3)_2PO_4$ compound (labels of atoms are given in Fig. 10)

Interacting atoms	Fe–O–P/°	P–O–Fe/°
Fe(2)–O(3)–P(2)–O(5)–**Fe(2)**	130.6	134.4
Fe(2)–O(4)–P(3)–O(7)–**Fe(1)**	144.6	133.1
Fe(2)–O(5)–P(2)–O(9)–**Fe(1)**	134.4	164.7

References

1 G. Férey and A. K. Cheetham, *Science*, 1999, **283**, 1125.
2 A. K. Cheetham, G. Férey and T. Loiseau, *Angew. Chem., Int. Ed.*, 1999, **38**, 3268.
3 M. Riou-Cavellec, D. Riou and G. Férey, *Inorg. Chim. Acta*, 1999, **291**, 317.
4 P. B. Moore and J. Shen, *Nature*, 1983, **306**, 356.
5 D. R. Corbin, J. F. Whitney, W. C. Fultz, G. D. Stucky, M. M. Eddy and A. K. Cheetham, *Inorg. Chem*, 1986, **25**, 2280.
6 H. M. Lin, K. H. Lii, Y. L. Jiang and S. L. Wang, *Chem. Mater.*, 1999, **11**, 519.
7 A. Choudhury, S. Natarajan and C. N. R. Rao, *Chem. Mater.*, 1999, **11**, 2316.
8 Z. A. D. Lethbridge and P. Lightfoot, *J. Solid State Chem.*, 1999, **143**, 58.
9 A. Choudhury, S. Natarajan and C. N. R. Rao, *J. Solid State Chem.*, 1999, **146**, 538.
10 J. R. D. Debord, W. M. Reiff, C. J. Warren, R. C. Haushalter and J. Zubieta, *Chem. Mater.*, 1997, **9**, 1994.
11 H. Li, A. Laine, M. O'Keefe and O. M. Yaghi, *Science*, 1999, **283**, 1145.
12 C. Trobajo, A. Espina, E. Jaimez, S. A. Khainakov and J. R. García, *J. Chem. Soc., Dalton Trans.*, 2000, 787.
13 M. J. Wilson and D. C. Bain, *Mineral. Mag.*, 1986, **50**, 291.
14 O. V. Yakubovich and M. S. Dadashov, *Kristallografiya*, 1992, **37**, 1403.
15 M. Cavellec, D. Riou and G. Ferey, *Acta Crystallogr., Sect. C*, 1994, **50**, 1379.
16 M. A. Salvadó, P. Pertierra, S. García-Granda, A. Espina, C. Trobajo and J. R. García, *Inorg. Chem.*, 1999, **38**, 5944.
17 O. V. Yakubovich, *Kristallografiya*, 1993, **38**, 43.
18 O. V. Yakubovich and M. S. Dadashov, *Sov. Phys. Crystallogr.*, 1992, **37**, 757.
19 P. B. Moore, *Am. Mineral.*, 1966, **51**, 168; J. Borensztajn, *Bull. Soc. Fr. Mineral. Cristallogr.*, 1966, **89**, 428.
20 S. M. Stalder and A. P. Wilkinson, *J. Mater. Chem.*, 1998, **8**, 261.
21 I. Vencato, E. Mattievich, L. F. Moreira and Y. P. Mascarenhas, *Acta Crystallogr., Sect. C*, 1989, **45**, 367.
22 J. R. Pilbrow, *Transition Ion Electron Paramagnetic Resonance*, Clarendon Press, Oxford, 1990.
23 A. Abragam and B. Bleaney, *Electron Paramagnetic Resonance of Transition Ions*, Dover Publications, New York, 1986.
24 R. L. Carlin and A. J. Van Duyneveldt, *Magnetic Properties of Transition Metal Compounds*, Springer-Verlag, Berlin, 1977.
25 A. Goñi, L. Lezama, N. O. Moreno, L. Fournès, R. Olazcuaga, G. E. Barberis and T. Rojo, *Chem. Mater.*, 2000, **12**, 62.
26 B. Bazán, J. L. Mesa, J. L. Pizarro, L. Lezama, M. I. Arriortua and T. Rojo, *Inorg. Chem.*, 2000, **39**, 6056.
27 A. B. Vassilikou-Dova and G. Lehmann, *Fortschr. Mineral.*, 1987, **65**, 173.
28 J. B. Goodenough, in *Magnetism and the Chemical Bond*, Interscience, New York, 1963.
29 M. Cavellec, G. Férey and J. M. Greneche, *J. Magn. Magn. Mater.*, 1997, **167**, 57.